

INCREASED AMPLIFIER SPACING USING QUANTUM WELL SATURABLE ABSORBERS AND SPECTRAL FILTERING IN A SOLITON SYSTEM

D. Atkinson, W.H. Loh†, V.V. Afanasjev‡, A.B. Grudinin†, A.J. Seeds and D.N. Payne†

*Optoelectronics Research Centre, Department of Electronic and Electrical Engineering,
University College London, Torrington Place, London WC1E 7JE, UK.*

†*Optoelectronics Research Centre, University of Southampton, Southampton SO9 5NH, UK.*

‡*General Physics Institute, 38 Vavilov Street, 117942 Moscow, Russia.*

Abstract

Passive MQW saturable absorbers and narrow-band filters permit 100km optical amplifier spacings in a proposed soliton system. After 9000km at 10Gbit/s, soliton-soliton interactions and Gordon-Haus jitter yield BER better than 10^{-9} .

There has been growing interest in the use of soliton systems incorporating optical amplifiers for high bit-rate, long distance telecommunications. However, with no soliton control, system performance is degraded both by the interaction with amplifier spontaneous emission noise, leading to Gordon-Haus (GH) timing jitter [1], and by soliton-soliton interactions [2]. Active soliton control in the time and frequency domains using synchronous modulation has shown enhanced performance [3]. Narrow-band filtering alone can reduce both GH jitter [4] and soliton-soliton interactions; however, filtering and amplification leads to the formation of low-level non-soliton radiation that interacts detrimentally with the solitons. This interaction can be suppressed by the use of sliding filters [5]. Alternatively, the introduction of non-linear gain, or saturable absorption (SA), can preferentially suppress the non-soliton radiation [6,7] and give unlimited stable soliton propagation [8]. Recently the use of filtering and non-linear gain using non-linear loop mirrors has been investigated [9].

For all the above schemes, the amplifier separation is of the order 50km or less, though Ref. [10] has shown that 100km is possible with active control. In this paper we demonstrate theoretically the use of identical narrow-band pass filters and passive, multiple quantum well (MQW) saturable absorbers as a means of significantly increasing the spacing between amplifiers to 100km whilst still achieving better than 10^{-9} bit-error rates after transmission over 9000km at 10Gbit/s. The component arrangement is depicted schematically in Fig. 1. and repeated along the 9000km span.

At normal incidence, InP based MQW material offers a compact, polarisation insensitive, fast saturable absorber on a low loss substrate. The loss change on saturation and hence the suppression of the low-level radiation relative to the solitons, can be increased simply by increasing the number of quantum wells (at the expense of requiring greater pulse powers); furthermore, this control can be applied at each amplifier.

In the SA model [11], photogenerated excitons decay with a fast time constant, τ_f , to free carriers, which in turn recombine with a slower time constant τ_s . Both free carriers and excitons (with normalised densities x and y respectively) screen absorption resulting in a time and intensity dependent absorption coefficient $\alpha(I, t)$. We use a Runge-Kutta method to solve the equations below [11];

$$\frac{dx}{dt} = \frac{2\bar{\alpha}I}{\tau_s I_s} - \frac{x}{\tau_f}, \quad \frac{dy}{dt} = \frac{1}{2} \frac{x}{\tau_f} - \frac{y}{\tau_s}$$

where $\bar{\alpha} = 1 - x - y$; under cw illumination, $\bar{\alpha} = 1/2$ when $I = I_s$. Using the small signal absorption coefficient α_0 , we obtain $\alpha(I, t) = \bar{\alpha}\alpha_0$.

Typical MQW parameters [12] are $\alpha_0 \approx 10^4 \text{cm}^{-1}$, $\tau_f \approx 300\text{fs}$, $\tau_s \approx 1\text{ns}$, $I_s \approx 2\text{kW/cm}^2$, though I_s can be varied considerably through barrier design. To discriminate low-level radiation from solitons we require a saturation intensity comparable to the soliton peak intensity ($\approx 130\text{kW/cm}^2$ for 38mW peak power focussed into $30\mu\text{m}^2$). We also require near complete

recovery of the unsaturated absorption in a time scale shorter than the 100ps inter pulse spacing for 10Gbit/s operation. Lifetimes of the order ps can be obtained from low-temperature molecular beam epitaxy grown material [13]. Alternatively, the free carriers can be swept out of the QW region using a DC electrical bias. With a saturated drift velocity of $\approx 10^7$ cm/s, carriers can be removed from an intrinsic region of $1\mu\text{m}$ thickness in 10ps. Reduction of the free carrier lifetimes will result in a corresponding increase in saturation intensity and in this model we use $\tau_s = 10\text{ps}$ and $I_s = 200\text{kW}/\text{cm}^2$. Using biased devices with different barrier structures, Wood *et al.*[14] have observed values of I_s both greater and less than $200\text{kW}/\text{cm}^2$. Lower values can be accommodated by using a larger spot size. Figure 2 plots the calculated response of the saturable absorber to the initial pulse with full width half maximum T_{FWHM} 15ps and peak intensity $127\text{kW}/\text{cm}^2$. The other parameters are $\tau_f = 300\text{fs}$ and $\alpha_0 d = 0.4$ where d is the total quantum well thickness and corresponds to 50-100 wells, depending on α_0 .

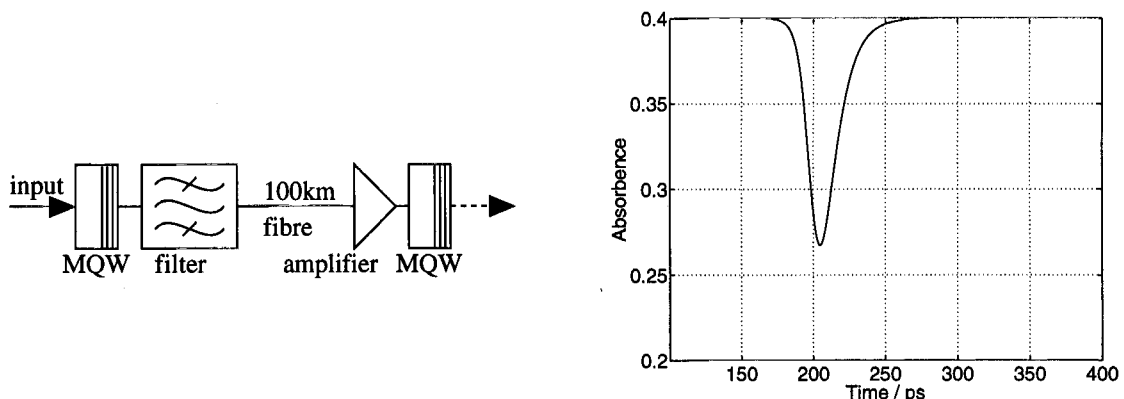


Fig. 1. (left) Schematic showing the order of components.

Fig. 2. (right) Absorbance $\alpha(I, t)d$, as pulse centred at 200ps, passes through the MQW.

Intensity and time dependent absorption changes $\Delta\alpha(I, t)$, lead to refractive index changes $\Delta n(I, t)$ and a subsequent chirping of the soliton. We use the relationship $\Delta n(I, t) = C\Delta\alpha(I, t)$, where C is taken as $2.4 \times 10^{-7}\text{m}$ (corresponding to an effective linewidth enhancement factor [15] of 2) and $\Delta\alpha(I, t) = \alpha(I, t) - \alpha_0$. In reality C is wavelength and intensity dependent, however to simplify our model we keep C constant but choose a value from the index changes observed by Ehrlich *et al.* [16] ($\Delta n = -0.12, \Delta\alpha = -5000\text{cm}^{-1}$) which are larger than most calculated changes.

The filter has amplitude transmission function [7] $H(f) = (1 + 2if/B)^{-1}$, where f is the frequency relative to the initial pulse centre frequency and we choose $B = 60\text{GHz}$. Propagation in the fibre was modelled using the split-step Fourier method [17] to solve the non-linear Schrödinger equation. The fibre parameters used were, dispersion $D = 0.45\text{ps}/(\text{nm}\cdot\text{km})$, loss $0.23\text{dB}/\text{km}$, nonlinear index coefficient $n_2 = 2.7 \times 10^{-20}\text{m}^2\text{W}^{-1}$, effective core area $A_{\text{eff}} = 50\mu\text{m}^2$ and operating wavelength, λ , of 1557nm . A constant linear time shift of $0.0366\text{ps}/\text{km}$ has been applied to the pulse to compensate for the effective first order dispersion introduced by the filter, saturation process and chirp. Pulses with peak power P_0 of 38mW and width T_{FWHM} of 15ps , are launched with the form $P_0 \text{sech}^2(\tau/\tau_0)$ where $\tau_0 = T_{\text{FWHM}}/1.76$. In this simulation the amplifiers maintain the total pulse energy constant. We note that this requires the gains of the amplifiers to change by not more than 0.1dB .

In the absence of the saturable absorber, Figure 3 shows the solitons are unstable and break up with 100km amplifier spacing (note, for the parameters used here the dispersion length is 125km). With the saturable absorber, Figure 4 demonstrates that soliton propagation becomes stable over 9000km . The stability is not sensitive to the chirp imparted by the index changes in the saturable absorber. We have observed stable propagation with the sign of the index change reversed and with no index changes ($C = 0$). The pulse is not a true soliton in the lossy fibre

and this generates chirp which is generally larger than the saturable absorber induced chirp. At 5000km, the FWHM of the pulses after each amplifier is 15.6ps; when $C = 0$, this FWHM is 14.4ps, indicating that in this filtered system the SA's contribution to the pulse chirp is relatively minor. The change in time of refractive index (proportional to the absorbence plotted in Fig. 2.) is asymmetric and introduces a frequency shift on the pulse, this has previously been observed in semiconductor optical amplifiers [18]. The narrow-band filters limit this frequency shift. Following amplification, the SA action decreases the pulse width from 15.6ps to 15.3ps, the filter reduces pulse chirp and increases its temporal width to 17.2ps, the pulse then narrows over the first 70km of fibre to 14.4ps, before broadening to 15.6ps at the end of the 100km fibre.

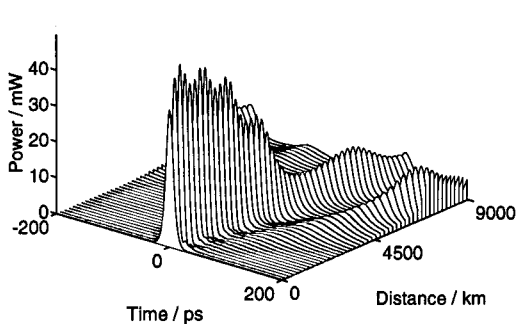


Fig. 3. (left) Pulse at launch and after every second amplifier with filters but no saturable absorbers.

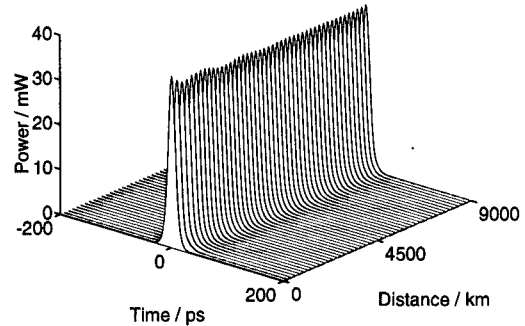


Fig. 4. (right) As Fig. 3. but with saturable absorbers.

Figure 5 shows the effect of propagating two solitons, initially in phase with separation 100ps, corresponding to a bit rate of 10Gbit/s. After 9000km, soliton-soliton interactions lead to a pulse peak separation of 101.5ps. To calculate the GH timing jitter, each amplifier introduces on the pulse a random frequency shift with variance $\langle \bar{\Omega}^2 \rangle$ given by [19];

$$\langle \bar{\Omega}^2 \rangle = \frac{(2\pi c)^2 \hbar n_2 N_{sp} (G - 1)}{3\tau_0 D \lambda^4 A_{eff} Q}$$

where N_{sp} is taken to be 1.0, G is the amplifier gain and Q is P_0/P_f , P_f being the peak power of the fundamental soliton (3.7mW here). Figure 6 plots the standard deviation of pulse positions with no filtering or SA [19] and the result of 100 trials of our model. The pulse positions T are determined using $T = \int |\psi|^2 t dt / \int |\psi|^2 dt$ where ψ is the pulse amplitude. After 9000km, the standard deviation of the jitter is only 2ps. For a bit error rate of 10^{-9} the pulse jitter should be less than $50\text{ps}/6.1 = 8\text{ps}$ for 10Gbit/s operation[1]. The mean power after each amplifier, assuming an equal proportion of 1's and 0's, is 5dBm.

Finally, the above results are not very sensitive to various system parameters as was found through repeated simulations altering only one parameter at a time. The filter was replaced with a filter having a \cos^2 power transmission, with free spectral range 120GHz, in another run the lifetime τ_s was reduced to 1ps and in a further trial the saturation intensity I_s was reduced to $20\text{kW}/\text{cm}^2$. In each case we obtained stable propagation for the 38mW, 15ps input pulse. The soliton-soliton interactions lead to a pulse separation different from 100ps by less than 2ps and a timing jitter standard deviation less than 2ps.

In summary, MQW material offers a compact, polarisation insensitive, passive saturable absorber. In combination with narrow band filtering we have demonstrated theoretically their use in a soliton system to increase the amplifier spacing to 100km. For a long-haul system of 9000km operating at 10Gbit/s with mean power only 5dBm, the effects of soliton-soliton interactions and Gordon-Haus jitter yield bit error rates better than 10^{-9} .

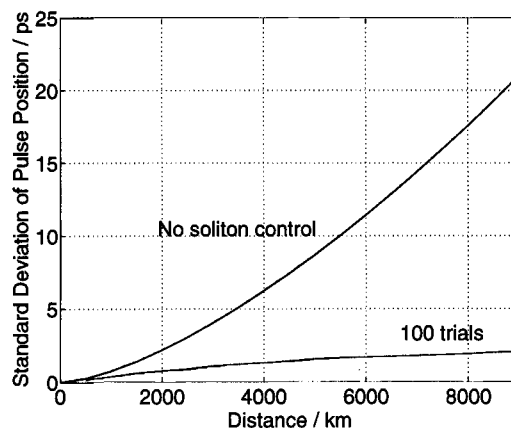
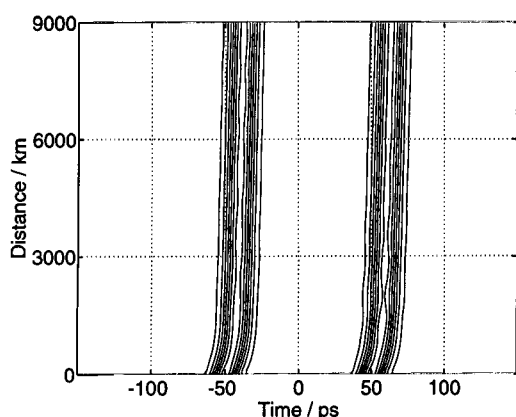


Fig. 5. (left) Contour plot showing little interaction between two solitons.
Fig. 6. (right) Gordon-Haus limit and the jitter observed after 100 trials.

References

1. J.P. Gordon and H.A. Haus, *Opt. Lett.***11**, 665 (1986).
2. F.M. Mitschke and L.F. Mollenauer, *Opt. Lett.***12**, 355 (1987).
3. M. Nakazawa, K. Suzuki, E. Yamada, H. Kubota, Y. Kimura and M. Takaya, *Electron. Lett.* **29**, 729 (1993).
4. A. Mecozzi, J.D. Moores, H.A. Haus and Y. Lai, *Opt. Lett.***16**, 1841 (1991).
5. L.F. Mollenauer, E. Lichtman, M.J. Neubelt and G.T. Harvey, *Electron. Lett.* **29**, 910 (1993).
6. Y. Kodama, M. Romagnoli and S. Wabnitz, *Electron. Lett.* **28**, 1981 (1992).
7. Y. Kodama, M. Romagnoli, S. Wabnitz and M. Midrio, *Opt. Lett.***19**, 165 (1994).
8. V.V. Afanasjev, W.H. Loh, A.B. Grudinin, D. Atkinson and D.N. Payne. Paper CThN1 to be presented at CLEO, Anaheim, USA. , 1994.
9. M. Matsumoto, H. Ikeda and A. Hasegawa, *Opt. Lett.***19**, 183 (1994).
10. H. Kubota and N. Nakazawa, *Electron. Lett.* **29**, 1780 (1993).
11. H.A. Haus and Y. Silberberg, *J. Opt. Soc. Am.* **B2**, 1237 (1985).
12. J.S. Weiner, D.B. Pearson, D.A.B. Miller, D.S. Chemla, D. Sivco and A.Y. Cho, *Appl. Phys. Lett.***49**, 531 (1986).
13. S. Gupta, J.F. Whitaker and G.A. Mourou, *IEEE J. Quantum Electron.* **28**, 2464 (1992).
14. T.H. Wood, T.Y. Chang, J.Z. Pastalan, C.A. Burrus Jr, N.J. Sauer and B.C. Johnson, *Electron. Lett.* **27**, 257 (1991).
15. C.H. Henry, *IEEE J. Quantum Electron.* **18**, 259 (1982).
16. J.E. Ehrlich, D.T. Neilson, A.C. Walker and M. Hopkinson, *Opt. Commun.***102**, 473 (1993).
17. G.P. Agrawal, *Nonlinear Fiber Optics* (Academic Press 1989).
18. N.A. Olsson and G.P. Agrawal, *Appl. Phys. Lett.***55**, 13 (1989).
19. D. Marcuse, *J. Lightwave Technol.* **10**, 273 (1992).